

File ID 73718  
Filename CHAPTER 6 The Influence of Specimen Attachment and Dimension on the  
Microtensile Strength

---

SOURCE (OR PART OF THE FOLLOWING SOURCE):

Type Dissertation  
Title Esthetic and bonding enhancements of tooth colored indirect restorations  
Author A.A. El-Zohairy  
Faculty Faculty of Dentistry  
Year 2004

FULL BIBLIOGRAPHIC DETAILS:

<http://dare.uva.nl/record/158138>

---

*Copyright*

*It is not permitted to download or to forward/distribute the text or part of it without the consent of the author(s) and/or copyright holder(s), other than for strictly personal, individual use.*

---

---

## CHAPTER 6

### The Influence of Specimen Attachment and Dimension on the Microtensile Strength

---

#### 6.1 Abstract

The higher microtensile bond strength values found for specimens with a smaller cross-sectional area are often explained by the lower occurrence of internal defects and surface flaws. We hypothesized that this aberrant behavior is mainly caused by the lateral way of attachment of the specimens to the testing device, which makes the strength dependent on the thickness. This study showed that composite bars of 1x1x10, 1x2x10, and 1x3x10mm attached at their 1 mm wide side (situation A) fractured at loads of the same magnitude, as a result of which the microtensile strength ( $\mu$ TS) calculated as  $F/A$  (force at fracture/cross-sectional area) significantly increased for specimens with decreasing thickness. Attachment at the 1, 2, or 3mm wide sides (situation B) resulted in equal  $\mu$ TS-values ( $P > 0.05$ ). Finite Element Analysis showed different stress patterns for situation A, but comparable patterns for situation B. Both situations showed the same maximum stress at fracture.

## 6.2 Introduction

The bond strength of restorative materials to the dental hard tissues is usually reported as the load at failure divided by the cross sectional area of the bonded interface ( $F/A$ ). Strength values calculated in this way are referred to as the "nominal strength" values, but this is only valid if the applied load is equally distributed throughout the entire bonded interface. Therefore, a crucial factor in evaluating the usefulness of a specific bond strength test is a thorough awareness of the stress patterns, which are involved in bond failure. Finite element analysis (FEA) studies have demonstrated that the manner in which loads are generally applied in the shear test or tensile bond strength tests, results in non-uniform stress patterns.[1] With shear loading severe stress concentrations arise near the loading site [2] as well as tensile stresses caused by a bending moment.[3] With the tensile bond strength test, where specimens are pulled away from a larger flat surface, there are pronounced stress concentrations at the periphery of the interface due to the change in the geometry and material properties of the materials bonded together.[1] These stress concentrations could explain the frequent cohesive failures within the substrate and the discrepancy between the actual nominal strength of the substrate and the apparent low stress measured.[4-6] Stress inhomogeneities due to geometry differences can be reduced significantly by bonding two-rod specimens of uniform cross-section together and by pulling them at the top and bottom surfaces.[7] The specimens used in the microtensile bond strength test ( $\mu$ TBS test) [8] have a uniform geometry at the bonding interface as well, but the tensile load in most investigations is not applied at top and bottom surfaces. Rectangular bar shaped specimens are commonly attached by sticking them to one of their flat lateral sides to the test set-up. Hourglass shaped specimens either with a cylindrical or a rectangular bonding area [9] are mounted by means of special designed holders enclosing the specimens. Some of these studies showed an inverse relationship between the  $\mu$ TBS and specimen size [8] and the higher values found for specimens with a smaller cross-sectional area were explained by a lower occurrence of internal defects and surface flaws. However, till now the aspect of lateral attachment, as a possible cause for the inverse relationship, has not been taken into consideration. We hypothesized that this inverse relationship is mainly caused by the lateral way of attachment to the testing device, which makes the strength dependent on the thickness of the specimens. The hypothesis was tested by determining the microtensile strength ( $\mu$ TS) of rectangular composite bars by varying the width at the attachment site and the thickness, and to determine with FEA the stress patterns involved.

### 6.3 Materials and methods

#### *Specimen preparation*

Composite (Synergy, Coltène, Altstätten, CH) was incrementally built-up in layers to produce blocks of approximately 15x10x10 mm. Each layer was light cured for 40 s using the Optilux 501 (Kerr, Danbury, CT, USA) at 700 mW/cm<sup>2</sup>. Three blocks were prepared and stored in distilled water at 37 °C for 1 day and subsequently cut into slabs of 1 mm thickness using a low-speed water-cooled saw (Buehler Isomet 1000, Buehler Ltd, Lake Bluff, IL, USA). Each block was then rotated 90(±1)° and again sliced to gain rectangular bars with 3 different widths of 1, 2 and 3 mm. The bars were cut-off at a length of 10 mm and distributed in equal numbers to five test groups and directly tested.

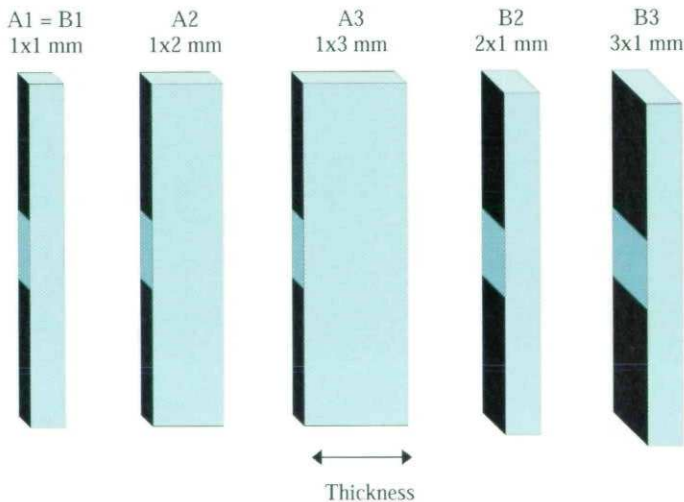


**Figure 6.1** The five different ways of attachment of the composite bars to the testing device. The upper and lower black surfaces indicate the sites that were bonded, each occupying 4mm in length. The gauge length (middle part) was 2mm.

#### *Micro Tensile Strength Test*

The  $\mu$ TS of the bars was determined in a universal testing machine (Instron, High Wycombe, Bucks, UK) at a crosshead speed of 1 mm/min. The specimens were attached with their lateral sides to the test set-up (Figure 3.1) with a dental adhesive (Clearfil SE Bond, Kuraray Co., Japan). The  $\mu$ TS of each composite bar was calculated by dividing the force at failure by its cross-sectional area. Two situations were evaluated. Situation A comprised groups A1, A2 and

A3 with bars of respectively 1x1x10, 1x2x10 and 1x3x10 mm, which were attached at their 1 mm wide side. Situation B comprised groups B1 (= A1), B2 and B3 where the bars were attached at their 1, 2 or 3 mm wide side (Figure 6.1).

One-way analysis of variance (ANOVA) was used to determine differences in  $\mu$ TS between the five groups. The comparison was analyzed with the Bonferroni post hoc analysis.  $P < 0.05$  was considered significant.

#### *Finite Element Analysis (FEA)*

To reveal the stress distribution in the composite bars an FEA was carried out with FEMAP 8.10 (ESP, Maryland Height, MO) and CAEFEM 7.3 (CAC, West Hills, CA). Three-dimensional models were created according to the different specimen dimensions as tested in the  $\mu$ TS test. The models were 10 mm long with cross sectional areas of 1, 2 and 3 mm<sup>2</sup>. In accordance to the way of attachment of the specimens to the test set-up, the stationary and moving part of the stainless steel test set-up were at the lateral side of the models, each occupying 4 mm of the length, leaving the middle part of 2 mm free. The nodes of the lateral side of the stainless steel parts of 1 mm thickness were fixed for the upper part (no translation or rotation in any direction) and pinned for the lower part (no translation in the X and Y direction, cross sectional plane). The models with cross sectional areas of 1, 2 and 3 mm<sup>2</sup> were composed of 2250, 3500, and 4750 elements respectively. The elements, all equal in size, were solid brick elements with mid-side nodes that matched well to the three-dimensional analysis. Material properties were assumed to be isotropic, homogenous and linear-elastic and the attachment of the specimen to the stainless steel test setup was assumed to be rigid. Typical values for the Young's module and Poisson's ratio of 16.6 GPa and 0.24 respectively for the resin composite [10] and 190 GPa and 0.34 for the stainless steel [11] were used in the FEA. For each model the loads that were applied at the nodes at the lateral side of the lower stainless steel part were the corresponding loads at fracture (Table 6.1). As a control an additional three-dimensional case for 1x1, 1x2 and 1x3mm composite bars was run for attachments at the top and bottom surfaces, instead of at the lateral surface. The loads that were applied were as those for the A1=B1, A2, A3, B2, and B3 models (Figure 6.2).

To study whether the results could be generalized to other materials of different properties, the stress distribution patterns were also analyzed for all groups with Young's moduli of 5 and 120 GPa and a Poisson ratio of 0.24, and a Young's modulus 16.6 GPa and a Poisson ratio of 0.40.

## 6.4 Results

For situation A, where the specimens had a constant width of 1mm at the attachment site, but a variable thickness of 1, 2 or 3 mm, the  $\mu$ TS significantly decreased in the order A1→A2→A3 ( $P < 0.05$ ). For situation B, where the attachment widths were varied (1, 2 and 3 mm) and the thickness was kept constant at 1 mm, there was no difference between the  $\mu$ TS for groups B1 (=A1), B2 and B3 ( $P > 0.05$ ) (Table 6.1).

**Table 6.1** Mean load at fracture, microtensile strength ( $\mu$ TS) and standard deviations between brackets of the resin composite bars determined for various ways of attachment to the test set-up.

Group (each n=10)	Attachment width	Thickness	Load at fracture (N)	$\mu$ TS (MPa)
A3	1 mm	3 mm	57.0 (13.1)	19.0 <sup>c</sup> (4.2)
A2	1 mm	2 mm	55.4 (16.7)	27.7 <sup>b</sup> (6.6)
A1=B1	1 mm	1 mm	44.3 (16.0)	44.3 <sup>a</sup> (11.5)
B2	2 mm	1 mm	77.4 (21.6)	38.7 <sup>a</sup> (9.4)
B3	3 mm	1 mm	109.5 (30.3)	36.5 <sup>a</sup> (8.7)

Same superscript letters indicate no difference ( $P > 0.05$ ).

The FEA models showed that stresses were localized at approximately 0.2 mm from the fixed sites with an average value of the maximum major principle stress of 64 MPa and progressively decreased towards the opposite free surface to reach 32, 15 and 8 MPa for A1, A2 and A3 respectively. The stress distribution patterns for groups B2 and B3 were nearly identical to that of group A1 (Figure 6.2).

The FEA for all groups with Young's moduli of 5 and 120 GPa and a Poisson ratio of 0.24 and a Young's modulus 16.6 GPa and a Poisson ratio of 0.40 showed maximum stresses with a value of 66, 56 and 67 MPa respectively with stress distribution patterns not different from the analyses with a Young's module of 16.6 GPa and a Poisson ratio of 0.24.

For the control groups where the attachment was at the top and bottom of the bars, the stress distributions patterns were for all models uniform and nearly equal to the applied stresses (Figure 6.2).

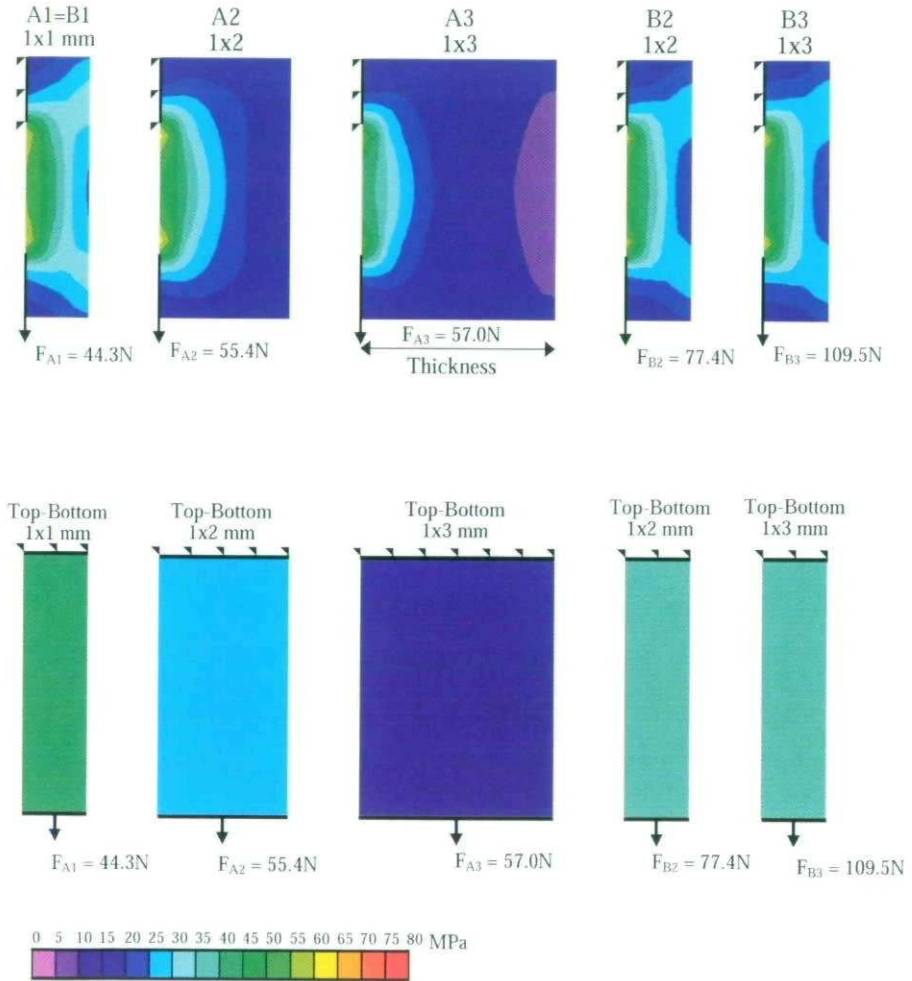


**Figure 6.2** Stress patterns in the middle 4mm for the models with lateral attachment (models in top row) and top and bottom attachment (models in bottom row). For each of the models A1=B1, A2, A3, B2, and B3 the applied loads were the loads at fracture (Table 6.1). These loads were also applied for top and bottom attachment (bottom row models). For lateral attachment maximum major principle stresses were localized at approximately 0.2 mm from the fixed sites: 70.8, 64.2, 56.0, 62.2, and 65.0 MPa for A1(=B1), A2, A3, B2, and B3 respectively. For top and bottom attachment the major principle stresses were 44.3, 27.7, 19.0, 38.7, and 36.5 MPa respectively. The triangles and arrows indicate the stationary and moving sides of the models respectively.

## 6.5 Discussion

The results of this study demonstrated a clear dependence of the  $\mu$ TS on the thickness of rectangular composite bars. The thinner the specimens became (A3→A2→A1), the higher were the values for the  $\mu$ TS (Table 6.1). This inverse relationship arises, as the loads at fracture for A1, A2, and A3 (Table 6.1) were of the same magnitude, while the cross-sectional area decreased ( $3\text{mm}^2 \rightarrow 2\text{mm}^2 \rightarrow 1\text{mm}^2$ ), therefore the  $\mu$ TS ( $F/A = \text{fracture load/cross-sectional area}$ ) becomes higher. The rationale for this inverse relationship between the  $\mu$ TS and thickness can be obtained from the FEA models. These showed that with lateral attachment the resultant stresses were not uniformly distributed and that stress concentration near the points of specimen fixation to the test set-up occurred with approximately the same magnitude (Figure 6.2); the pattern of stress distribution improved when the thickness of the specimens decreased *i.e.* when the distance between load path and free opposite surface became less eccentric. Increasing the width of specimen fixation with keeping the thickness constant at 1 mm had almost no effect on the stress distribution patterns. These stress patterns were quite similar to those of A1(=B1) and as a result the  $\mu$ TS of the specimens were similar.

The sensitivity of the  $\mu$ TS to changes in specimen thickness when specimens are attached at a lateral side to the test set-up will also be encountered with the microtensile bond strength ( $\mu$ TBS). Indeed a similar dependence was found for the  $\mu$ TBS with hourglass shaped specimens that were attached at the lateral side [8] and with cylindrical and rectangular hour-glass shaped specimens, that were mounted in special designed holders that provided the support and load application positioned at the shoulders of the hourglass.[9] The lower maximum principle stress in specimens with the smallest cross-sectional area as found in the latter study is not contradictory to the present study where for these specimens this stress was the highest. It should be noted that in the FEA of the latter study loads were applied that produced an average tensile stress, which was the same (20 MPa) for all sizes of specimens. In the present study the fracture loads were applied to the models to produce average tensile stresses, which corresponded to the average  $\mu$ TS for each of the five groups.

The most effective way to avoid inhomogeneous stress distributions is by applying the loads and the support at the top and bottom surfaces of the specimens.[1] The FEA results of the control models where this was done showed for all models (1x1, 1x2 and 1x3 mm) that the generated stresses were uniform and equal to the applied stresses without any stress concentrations (Figure 6.2). Yet an inverse relationship between strength and specimen size can exist as a result of differences in the amount of flaws, which will be greater in number for

specimens with a larger cross-section.[8] The role of flaws could explain the differences in strength found between the 1, 2 and 3 mm<sup>2</sup> composite bars when the thickness was kept constant at 1 mm. Although the differences were not significant, the bars with larger cross-sectional areas tended to decrease in strength.

Important considerations in using a particular microtensile testing set-up are the ease of handling in producing the specimens and their way of attachment. However, in the existing test set-ups inhomogeneous stress distributions will always occur due to the way of mounting or attaching the specimens. Only with top and bottom attachment stress concentrations can be minimized or eliminated (Figure 6.2). This way of attachment may be feasible for the hourglass shaped specimens, but not for the straight bars, as they do not offer sufficient surface for adhesion to the test set-up to withstand the tensile forces applied during the test. The best option for straight bars for both the  $\mu$ TS and  $\mu$ TBS-test is yet to attach them at their lateral side to the test set-up with the smallest possible thickness, as this brings the free opposite surface closer to the path of load application, which would contribute to further leveling the stresses. The smallest dimension in thickness is limited by the cutting procedure, which should not cause premature fractures.

Although an inverse relationship between tensile strength and cross-sectional area was observed in the earlier mentioned studies [8,9], the present study has demonstrated that this is caused by lateral load application to the micro specimens, and we are now able to better understand "the phenomenon of inverse relationship". The hypothesis that the  $\mu$ TS is dependent on the thickness of the specimens when the attachment is at the sides of the specimens was therefore accepted. In addition, the FEA results showed that most probably a wide range of materials is equally sensitive to these mounting conditions although further tests are required for a sound prove.

## 6.6 References

- [1] Van Noort R, Noroozi S, Howard IC, Cardew G. A critique of bond strength measurements. *J Dent* 1989; 17: 61-67.
- [2] DeHoff PH, Anusavice KJ, Wang Z. Three-dimensional finite element analysis of the shear bond test. *Dent Mater* 1995; 11: 126-131.
- [3] Shiau JY, Rasmussen ST, Phelps AE, Enlow DH, Wolf GR. Analysis of the "shear" bond strength of pretreated aged composites used in some indirect bonding techniques. *J Dent Res* 1993; 72: 1291-1297.
- [4] Øilo G, Austrheim EK. In vitro quality testing of dentin adhesives. *Acta Odontol Scand* 1993; 51: 263-269.

- [5] Holtan JR, Nystrom GP, Olin PS, Phelps RA, 2nd, Phillips JJ, Douglas WH. Bond strength of six dentinal adhesives. *J Dent* 1994; 22: 92-96.
- [6] Versluis A, Tantbirojn D, Douglas WH. Why do shear bond tests pull out dentin? *J Dent Res* 1997; 76: 1298-1307.
- [7] Della Bona A, van Noort R. Shear vs. tensile bond strength of resin composite bonded to ceramic. *J Dent Res* 1995; 74: 1591-1596.
- [8] Sano H, Shono T, Sonoda H, Takatsu T, Ciucchi B, Carvalho R, Pashley DH. Relationship between surface area for adhesion and tensile bond strength--evaluation of a micro-tensile bond test. *Dent Mater* 1994; 10: 236-240.
- [9] Phrukkanon S, Burrow MF, Tyas MJ. The influence of cross-sectional shape and surface area on the microtensile bond test. *Dent Mater* 1998; 14: 212-221.
- [10] Craig RG, Powers JM. Mechanical properties. In. *Restorative dental materials*. Mosby, St. Louis, 2002. p. 78-79.
- [11] Shigley JE. In. *Mechanical engineering design*. McGraw-Hill, New York, 1980. p.

